ARMY RESEARCH LABORATORY

# Simulated Frequency and Force Modulation Atomic Force Microscopy on Soft Samples

**by Joshua C. Crone, Santiago Solares, and Peter W. Chung**

**ARL-TR-4166** **June 2007**

**Approved for public release; distribution is unlimited.**

## NOTICES

### Disclaimers

The findings in this report are not to be construed as an official Department of the Army position unless so designated by other authorized documents.

Citation of manufacturer's or trade names does not constitute an official endorsement or approval of the use thereof.

DESTRUCTION NOTICE—Destroy this report when it is no longer needed. Do not return it to the originator.

**Army Research Laboratory**
Aberdeen Proving Ground, MD 21005-5066

**ARL-TR-4166** **June 2007**

# Simulated Frequency and Force Modulation Atomic Force Microscopy on Soft Samples

**Joshua C. Crone and Peter W. Chung**
**Computational and Information Sciences Directorate, ARL**

**Santiago Solares**
**University of Maryland**

**Approved for public release; distribution is unlimited.**

# REPORT DOCUMENTATION PAGE

*Form Approved*
*OMB No. 0704-0188*

Public reporting burden for this collection of information is estimated to average 1 hour per response, including the time for reviewing instructions, searching existing data sources, gathering and maintaining the data needed, and completing and reviewing the collection information. Send comments regarding this burden estimate or any other aspect of this collection of information, including suggestions for reducing the burden, to Department of Defense, Washington Headquarters Services, Directorate for Information Operations and Reports (0704-0188), 1215 Jefferson Davis Highway, Suite 1204, Arlington, VA 22202-4302. Respondents should be aware that notwithstanding any other provision of law, no person shall be subject to any penalty for failing to comply with a collection of information if it does not display a currently valid OMB control number.
**PLEASE DO NOT RETURN YOUR FORM TO THE ABOVE ADDRESS.**

| | | |
|---|---|---|
| **1. REPORT DATE *(DD-MM-YYYY)*** June 2007 | **2. REPORT TYPE** Final | **3. DATES COVERED (From - To)** July 2006 to May 2007 |
| **4. TITLE AND SUBTITLE** Simulated Frequency and Force Modulation Atomic Force Microscopy on Soft Samples | | **5a. CONTRACT NUMBER** |
| | | **5b. GRANT NUMBER** |
| | | **5c. PROGRAM ELEMENT NUMBER** |
| **6. AUTHOR(S)** Joshua C. Crone (ARL); Santiago Solares (UM); and Peter W. Chung (ARL) | | **5d. PROJECT NUMBER** 7UH7CL |
| | | **5e. TASK NUMBER** |
| | | **5f. WORK UNIT NUMBER** |
| **7. PERFORMING ORGANIZATION NAME(S) AND ADDRESS(ES)** U.S. Army Research Laboratory<br>Computational and Information Sciences Directorate<br>Aberdeen Proving Ground, MD 21005-5066 | | **8. PERFORMING ORGANIZATION REPORT NUMBER** ARL-TR-4166 |
| **9. SPONSORING/MONITORING AGENCY NAME(S) AND ADDRESS(ES)** | | **10. SPONSOR/MONITOR'S ACRONYM(S)** |
| | | **11. SPONSOR/MONITOR'S REPORT NUMBER(S)** |

**12. DISTRIBUTION/AVAILABILITY STATEMENT**
Approved for public release; distribution is unlimited.

**13. SUPPLEMENTARY NOTES**

**14. ABSTRACT**

This report was generated as part of a Student Temporary Employment Program Internship from July 2006 through June 2007. The report presents basic didactic concepts and reviews recent progress in the scientific literature on atomic force microscopy (AFM). A new AFM technique is studied. The novel AFM approach is based on force and frequency modulation (FFM-AFM) that enables nondestructive AFM measurements of soft samples such as biological materials in solution. The vibrational properties of the AFM cantilever probe are examined to determine extremal conditions that the sample is likely to experience.

**15. SUBJECT TERMS**
band gap; crystals; modeling; photonics

| **16. SECURITY CLASSIFICATION OF:** | | | **17. LIMITATION OF ABSTRACT** | **18. NUMBER OF PAGES** | **19a. NAME OF RESPONSIBLE PERSON** Joshua C. Crone |
|---|---|---|---|---|---|
| **a. REPORT** Unclassified | **b. ABSTRACT** Unclassified | **c. THIS PAGE** Unclassified | SAR | 20 | **19b. TELEPHONE NUMBER** (*Include area code*) 410-278-6027 |

**Standard Form 298 (Rev. 8/98)**
**Prescribed by ANSI Std. Z39.18**

## Contents


**List of Figures** iv

**List of Tables** iv

**Acknowledgments** v

**1. Introduction** 1

**2. Tip Sample Interaction Forces** 2

**3. Frequency and Force Modulation-Atomic Force Microscopy (FFM-AFM)** 4

**4. Quantitative Prediction Tip Penetration and Repulsive Forces** 6

**5. Conclusions** 8

**6. References** 9

**7. Bibliography** 10

**Distribution List** 11

## List of Figures

Figure 1. Basic operation of an atomic force microscope (http://www.physics.ucsb.edu/~hhansma/afm-acs_news.htm). ..... 1

Figure 2. Illustrating the general shape of a force versus distance graph with the Lennard-Jones potential model (*1*). ..... 3

Figure 3. Illustration of bistability effect in AM-AFM. ..... 3

Figure 4. Tip broadening because the tip never reaches the true sample skin. ..... 4

Figure 5. Control scheme for FFM-AFM. ..... 5

Figure 6. Simulation of a triple-walled carbon nanotube imaging a bacteriorhodopsin molecule on a Si(100)-OH surface ..... 5

## List of Tables

Table 1. Base parameters used to investigate the correlation between AFM scanning parameters and tip penetration and repulsive forces. ..... 6

Table 2. Results from numerical simulations. ..... 6

Table 3. Results from numerical integration of equation 6. ..... 7

## Acknowledgments

The authors gratefully acknowledge partial support from the U.S. Army Research Laboratory's Major Shared Resource Center at the Computational & Informational Sciences Directorate, High Performance Computing Division, Computational Sciences & Engineering Branch through the Student Temporary Employment Program. Partial support is also gratefully acknowledged through the Joint Science and Technology Office of the Defense Threat Reduction Agency.

INTENTIONALLY LEFT BLANK

# 1. Introduction

As the focus of technology continues to become smaller, the need for tools to accurately image nanoscale samples continues to grow. A large step toward meeting this need occurred in the 1980s with the development of atomic force microscopy (AFM). With the invention of AFM, the ability to image samples on the atomic scale became more accurate and reliable. Over the past 20 years, numerous changes have been made in the different modes of operation and materials used during scanning. These changes have led to increased performance in atomic scale imaging and have consistently increased the potential applications of AFM. Along with determining surface topography of samples, AFM has been used to obtain information about the material and chemical properties of samples. The versatility in type of information gathered through AFM has made it one of the most effective tools in imaging on the atomic and nanoscale levels.

The atomic force microscope (see figure 1) is centered around a microscale cantilever beam that has a shape tip at the end. These tips are usually made of silicon or carbon nanotubes, depending on the desired application. Although each mode of operation varies, the basic principles are the same. The cantilever beam is excited at a certain amplitude and/or frequency. The interaction forces between the tip and the sample lead to changes in the amplitude, phase, or frequency of oscillation. Information can be obtained about the sample because of these changes. The motion of the cantilever beam, along with the changes in motion, is often determined by a diode laser reflected onto an array of photodiodes. The motion of the tip can be fit to a sine curve that informs the control loop of the amplitude, frequency, and phase of the cantilever at all times.

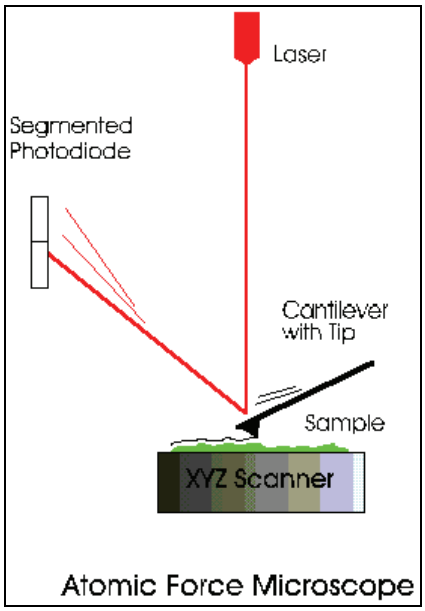


Figure 1. Basic operation of an atomic force microscope (http://www.physics.ucsb.edu/~hhansma/afm-acs_news.htm).

The governing equation for the vibration of the beam is given by

$$m\ddot{Z} + kZ + \frac{m\omega_o}{Q}\dot{Z} = F_{ts} + F_o \cos(\omega t). \tag{1}$$

This equation considers the cantilever-probe system as a point-mass spring system in which m is the mass of the cantilever, k is the cantilever force constant, $\omega_o$ is the free resonance frequency, Q is the quality factor, $F_{ts}$ is the tip-sample interaction forces, $F_o$ is the amplitude of the excitation force, ω is the frequency of the excitation force, Z is the height of the probe, and t is time.

## 2. Tip Sample Interaction Forces

As the tip or probe moves relative to the sample, it experiences varying forces. These forces include but are not limited to Van der Waals forces, mechanical contact forces, chemical bonding, electrostatic forces, and capillary forces. The tip-sample interaction forces depend on the type of tip used, the material of the type, and the material of the sample. These forces can be modeled in a number of ways such as with the Lennard-Jones potential, which is a relatively simple model representing the interaction between molecules. The force attributable to the Lennard-Jones potential, which is the negative gradient of the potential energy, is represented by

$$F(r) = 4\varepsilon\left(12\frac{\sigma^{12}}{r^{13}} - 6\frac{\sigma^{6}}{r^{7}}\right), \tag{2}$$

where r is the distance between molecules, ε is the depth of the potential well, and σ is the location of zero potential.

Figure 2 shows the shape of a Lennard-Jones force curve. When the tip and sample are far away from each other, there is a small attractive force. As the tip moves downward toward the sample, the force becomes more attractive until it reaches the maximum. As the tip continues to move down, the force becomes less attractive until it reaches the repulsive regime.

For the simulations in this work, the tip-sample interaction curves are determined through the calculation of the discrete atomic interactions. The energy of the system is calculated as a probe is lowered toward the sample at a fixed horizontal position. We find the force by taking the negative gradient of the energy, which is a function of the probe's distance from the sample. This force is then fit to equation 3 for use in the frequency and force modulation-ATM (FFM-AFM) simulation.

$$\begin{aligned} F &= \frac{-W}{1+30*(Z_{ts}-\sigma)} \quad \textit{for } Z_{ts} \geq \sigma \\ F &= -W + S*(Z_{ts}-\sigma)^2 \quad \textit{for } Z_{ts} \leq \sigma \end{aligned} \tag{3}$$

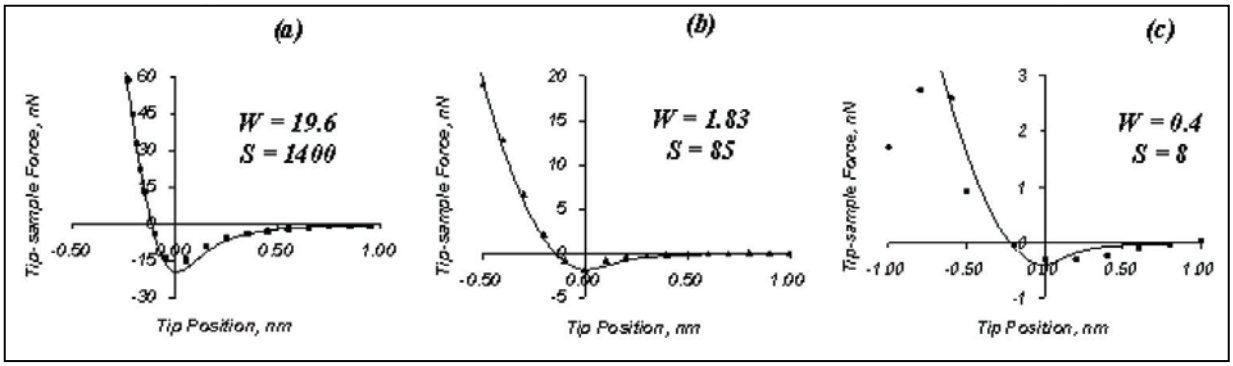


(a) 15-nm-radius silicon tip approaching a Si(100)-OH surface, (b) a 5.4-nm-radius single-walled carbon nanotube tip approaching a Si(100)-OH surface, and (c) a 2.4-nm-radius triple-walled carbon nanotube approaching a bacteriorhodopsin molecule

Figure 2. Illustrating the general shape of a force versus distance graph with the Lennard-Jones potential model (*1*).

In equation 3, $Z_{ts}$ represents the distance between the tip and sample, W is the maximum attractive force, σ is the location at which the maximum attractive force occurs, and S is the slope of the curve in the repulsive regime.

There are types of cantilever beam modulation approaches in AFM. One mode is amplitude modulation (AM-AFM) which is also referred to as tapping mode. In this mode, the cantilever is excited at or near resonance frequency at a height well above the sample. The cantilever is then lowered toward the sample while the excitation frequency and amplitude are kept constant. As the tip enters the repulsive regime, the effective amplitude of the tip decreases. The height of the sample is determined when the amplitude reaches a set point, which is defined before the experiment and is below the freely oscillating amplitude. There are two main weaknesses with this mode. The first is that it usually results in relatively high tip-sample interaction forces. This can lead to damage of the sample if the sample is too soft. The second is that it can also be subject to bistability which leads to inaccurate height measurements. Bistability occurs when the tip jumps from the attractive regime to the repulsive regime, and vice versa, as illustrated in figure 3.

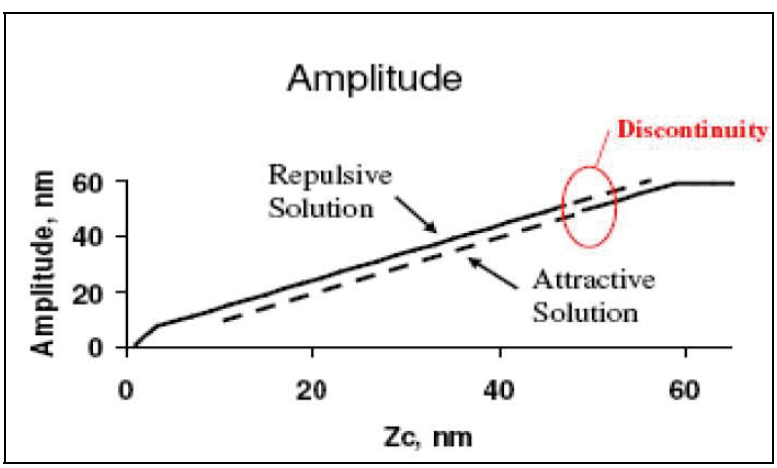


Figure 3. Illustration of bistability effect in AM-AFM.

The second common mode of imaging in AFM is frequency modulation-AFM (FM-AFM). In this mode, the excitation amplitude is kept constant but the excitation frequency is varied to match the current resonance frequency. This frequency changes because of the tip-sample interaction by

$$f = \sqrt{\frac{k - \nabla F_{ts}}{m}} \tag{4}$$

where $f$ is the current resonance frequency, k is the force constant, m is the mass of the cantilever, and $\nabla F_{ts}$ is the gradient of the tip-sample interaction forces over the range in which the tip is oscillating.

In FM-AFM, the tip height is decreased until the desired frequency shift is attained. The tip is then moved along the sample and continues to find the height that achieves the desired frequency shift. The amplitude of oscillation is much smaller than in AM-AFM. The weakness in this mode of AFM is that the small oscillations can have difficulties in imaging sharp topographical changes and the tip does not get as close to the sample, which may mean that a true scan is not achieved. This effect is often referred to as tip broadening and is shown in figure 4.

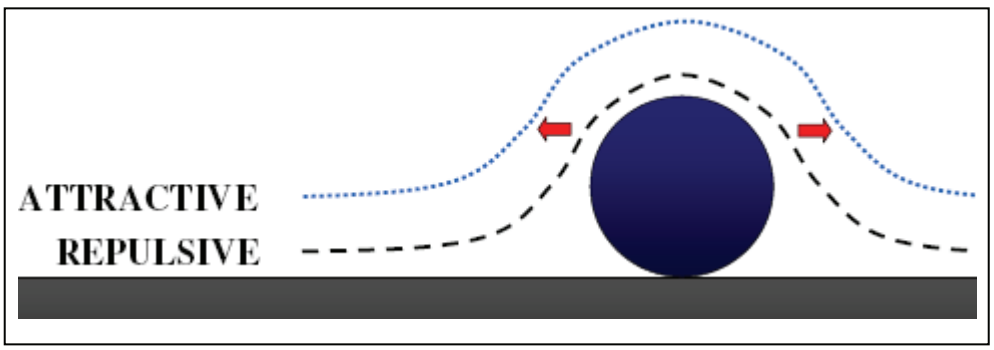


Figure 4. Tip broadening because the tip never reaches the true sample skin.

## 3. Frequency and Force Modulation-Atomic Force Microscopy (FFM-AFM)

Although multiple modes of AFM have been developed and numerous adaptations made, AFM still struggles to accurately image soft samples without causing permanent damage to the sample. In this proposed novel mode of AFM, the cantilever equilibrium position is kept constant. The excitation frequency is that of the current resonance frequency, as in FM-AFM. The excitation amplitude is varied until the frequency shift from the free resonance frequency is zero. At this point, the attractive and repulsive forces are equal. The sample height is then determined as the cantilever equilibrium minus the amplitude of oscillation. The cantilever sweeps horizontally across the sample, providing a real-time scan of the sample surface. The control scheme for FFM-AFM is depicted in figure 5.

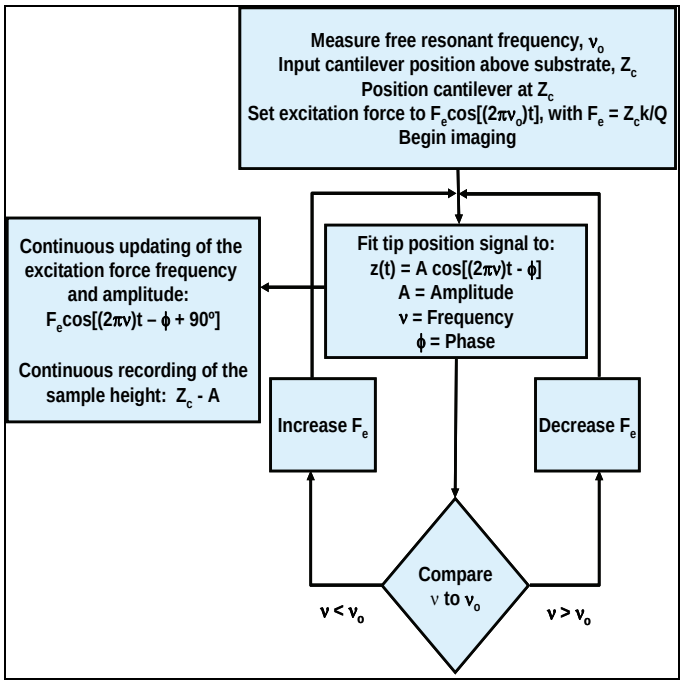


Figure 5. Control scheme for FFM-AFM.

FFM-AFM has many benefits over other AFM modes, especially in the scanning of soft samples such as biological materials. One advantage is that FFM-AFM limits the maximum repulsive force because of tip-sample interaction forces by limiting the frequency to no higher than the free resonance frequency. Figure 6 illustrates how the maximum repulsive force using FFM-AFM is less than that of AM-AFM. Another benefit is that bistability is eliminated because the excitation frequency is always the same as the current resonance frequency. A third advantage is that the control scheme includes only one control loop, meaning it should be a relatively simple method to implement.

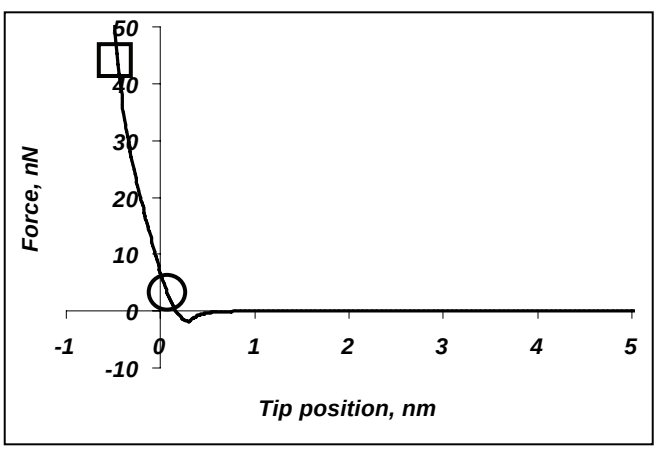


Figure 6. Simulation of a triple-walled carbon nanotube imaging a bacteriorhodopsin molecule on a Si(100)-OH surface. (The square indicates the maximum repulsive force experienced during AM-AFM imaging. The circle is the force experienced during FFM-AFM.)

## 4. Quantitative Prediction Tip Penetration and Repulsive Forces

The goal of this project is to quantitatively predict the maximum tip-sample repulsive forces and the maximum tip penetration, based on a proposed set of AFM scanning parameters. These parameters are the cantilever force constant k, the quality factor Q, the fixed equilibrium position of the cantilever Zc, and the free resonance frequency $w_o$. The free resonance frequency and force constant have an approximately linear relationship and therefore were varied together. We performed numerical simulations to model the imaging of a single scan point by performing numerical integration of the equation of motion (equation 1) using the Verlet algorithm to determine the velocity and position at each time step. After the beam achieves a zero frequency shift from the free resonance frequency, the maximum tip penetration is determined by the difference between the lowest point reached by the probe and the true height of the sample. The maximum interaction force can be calculated when this value is entered into equation 3.

The base parameters used for each run are listed in table 1. Table 2 shows the range used for each parameter and the resulting variation in tip-sample repulsive force and tip penetration as each AFM scanning parameter is varied.

Table 1. Base parameters used to investigate the correlation between AFM scanning parameters and tip penetration and repulsive forces.

| Parameter | Imaging in air | Imaging in water |
|---|---|---|
| Cantilever force constant, N/m | 2.5 | 2.5 |
| Cantilever free resonant frequency, kHz | 100 | 33 |
| Cantilever quality factor | 150 | 3 |
| Tip rest position above the substrate, nm | 10 | 10 |
| Well depth (for tip-sample interaction forces) | 0.5 | 0.5 |
| Steepness (for tip-sample interaction forces) | 5 | 5 |

Table 2. Results from numerical simulations.

| Parameter | Range | Maximum force over parameter range (nano-newton [nN]) | | Minimum force over parameter range (nN) | | Variation (percent) | |
|---|---|---|---|---|---|---|---|
| | | Air | Liquid | Air | Liquid | Air | Liquid |
| $Z_c$, nanometers (nm) | 5 to 50 | 0.658 | 0.652 | 0.637 | 0.638 | 3.3 | 2.2 |
| k, newtons per meter (N/m) | 0.5 to 50 | 0.669 | 0.670 | 0.639 | 0.598 | 4.8 | 11.9 |
| Q | 5 to 200 | 0.648 | 0.648 | 0.646 | 0.646 | 0.3 | 0.4 |

As seen in table 2, the AFM scanning parameters only have a small effect, if any, on the maximum tip-sample repulsive forces. The variation in the force constant showed the only real change and this resulted in a 0.07 nN difference in force. All forces are well below the critical level of 2.4 nN which would result in permanent damage to the sample (*1*). The variation on the tip penetration was negligible and remained between 0.47 and 0.48 nm.

The results of the numerical simulations suggest that these scanning parameters do not greatly affect the repulsive forces and tip penetration. This claim can be justified analytically if we examine the frequency shift equation from perturbation theory (*2*). This equation assumes the cantilever acts as a weakly perturbed harmonic oscillator. Although this assumption is only a true representation of the oscillating cantilever beam when the restoring force of the beam is significantly greater than the interaction forces, it is a good basis for analytical study. When we define $d+A_o$ as Zc and set the frequency shift to zero in equation 5, the equation simplifies to equation 6.

$$\Delta f = -\frac{1}{2\pi}\frac{\omega_o}{kA_o}\int_0^{2\pi} F_{ts}[d + A_o + A_o\cos(\varphi)]\cos(\varphi)d\varphi \tag{5}$$

$$0 = \int_0^{2\pi} F_{ts}[Z_c + A_o\cos(\varphi)]\cos(\varphi)d\varphi \tag{6}$$

As illustrated in equation 6, the frequency shift is not a function of the quality factor (Q). Also, the force constant (k) and the free resonance frequency ($\omega_o$) are removed because the frequency shift is zero. Therefore, it can be concluded that none of those three factors have an impact on the frequency shift and consequently, the maximum interaction forces. By performing numerical integration using the mid-point method with 10,000 intervals, while varying Zc, we can find the repulsive force. With this information, the tip penetration can also be determined. Table 3 contains the results of this integration. Both the repulsive force and tip penetration remain relatively small and unchanged except at an equilibrium height of 4 nm. The differences between these data and the results of the numerical simulations can be attributed to the fact that equation 5 assumes a weakly perturbed harmonic oscillator.

Table 3. Results from numerical integration of equation 6.

| | |
|---|---|
| W_depth | 0.5 |
| W_location | 3.4 |
| S | 5 |

| Zc | Ao | Zmin | Fts(Zmin) | Penetration | |
|---|---|---|---|---|---|
| 4 | 1.0240 | 2.9760 | 0.3991 | 0.4240 | |
| 5 | 2.0403 | 2.9597 | 0.4695 | 0.4403 | |
| 6 | 3.0462 | 2.9538 | 0.4953 | 0.4462 | |
| 7 | 4.0493 | 2.9507 | 0.5092 | 0.4493 | |
| 8 | 5.0513 | 2.9487 | 0.5182 | 0.4513 | |
| 9 | 6.0527 | 2.9473 | 0.5245 | 0.4527 | |
| 10 | 7.0537 | 2.9463 | 0.5293 | 0.4537 | |
| 11 | 8.0545 | 2.9455 | 0.5330 | 0.4545 | |
| 12 | 9.0552 | 2.9448 | 0.5360 | 0.4552 | |
| 13 | 10.0557 | 2.9443 | 0.5385 | 0.4557 | |
| 14 | 11.0562 | 2.9438 | 0.5406 | 0.4562 | |
| 15 | 12.0566 | 2.9434 | 0.5424 | 0.4566 | |
| 16 | 13.0569 | 2.9431 | 0.5440 | 0.4569 | |
| 17 | 14.0573 | 2.9427 | 0.5454 | 0.4573 | |
| 18 | 15.0575 | 2.9425 | 0.5466 | 0.4575 | |
| 19 | 16.0578 | 2.9422 | 0.5478 | 0.4578 | |
| 20 | 17.0580 | 2.9420 | 0.5487 | 0.4580 | |
| | | 1.15356 | 37.50489 | 8.0034 | **Percent Change** |
| | | 0.59948 | 16.87206 | 4.0052 | **Percent Change for Zc = 5-20** |

## 5. Conclusions

AFM is a powerful tool with numerous applications for the imaging and analysis of nanoscale samples. Despite the wide range of AFM methods, the imaging of soft samples is still limited. FFM-AFM is a mode of AFM that allows for the accurate scanning of soft samples without the risk of sample damage. FFM-AFM appears to be nearly independent of the AFM scanning parameters. More work is necessary to examine more parameter combinations and to begin determining more quantitative ways of comparing the AFM parameters to the tip penetration and tip-sample repulsive forces. A further investigation into other analytical methods to determine the correlation is also required.

## 6. References


1. Solares, Santiago D. Single Biomolecule Imaging With Frequency and Force Modulation in Tapping-Mode Atomic Force Microscopy. *Journal of Physical Chemistry B Letters* **2007**, submitted.

2. Garcia, R.; Perez, R. Dynamic Atomic Force Microscopy Methods. *Surface Science Reports* **2002**, *47*, 197-301.

## 7. Bibliography

1. Solares, Santiago D. Frequency and Force Modulation Atomic Force Microscopy: Low-Impact Tapping-Mode Imaging Without Bistability. *Measurement Science and Technology* **2007**, submitted.

| NO. OF COPIES | ORGANIZATION |
|---|---|
| 1 (PDF ONLY) | DEFENSE TECHNICAL<br>INFORMATION CTR<br>DTIC OCA<br>8725 JOHN J KINGMAN RD<br>STE 0944<br>FORT BELVOIR VA 22060-6218 |
| 1 | US ARMY RSRCH DEV & ENGRG CMD<br>SYSTEMS OF SYSTEMS<br>INTEGRATION<br>AMSRD SS T<br>6000 6TH ST STE 100<br>FORT BELVOIR VA 22060-5608 |
| 1 | DIRECTOR<br>US ARMY RESEARCH LAB<br>IMNE ALC IMS<br>2800 POWDER MILL RD<br>ADELPHI MD 20783-1197 |
| 1 | DIRECTOR<br>US ARMY RESEARCH LAB<br>AMSRD ARL CI OK TL<br>2800 POWDER MILL RD<br>ADELPHI MD 20783-1197 |
| 2 | DIRECTOR<br>US ARMY RESEARCH LAB<br>AMSRD ARL CS OK T<br>2800 POWDER MILL RD<br>ADELPHI MD 20783-1197 |
| 2 | DIRECTOR<br>US ARMY RESEARCH LAB<br>AMSRD ARL CI J GOWENS<br>R NAMBURU<br>2800 POWDER MILL RD<br>ADELPHI MD 20783-1197 |
| | ABERDEEN PROVING GROUND |
| 1 | DIRECTOR<br>US ARMY RSCH LABORATORY<br>ATTN AMSRD ARL CI OK (TECH LIB)<br>BLDG 4600 |
| 1 | DIRECTOR<br>US ARMY RSCH LABORATORY<br>ATTN AMSRD ARL CI H C NIETUBICZ<br>BLDG 328 |

| NO. OF COPIES | ORGANIZATION |
|---|---|
| 6 | DIRECTOR<br>US ARMY RSCH LABORATORY<br>ATTN AMSRD ARL CI HC J CLARKE<br>P CHUNG (5 CYS)<br>BLDG 394 |